

Preparation and phase transition of $\text{Gd}_4(\text{Al}_{1-x}\text{Ga}_x)_2\text{O}_9$ solid solutions

H. YAMANE*, T. SAKAMOTO, S. KUBOTA, M. SHIMADA
*Institute for Advanced Materials Processing, Tohoku University 2-1-1 Katahira,
 Aoba-ku, Sendai 980-8577, Japan*
E-mail: yamane@iamp.tohoku.ac.jp

The solid-solution compounds of $\text{Gd}_4(\text{Al}_{1-x}\text{Ga}_x)_2\text{O}_9$ ($x = 0.0\text{--}1.0$) were prepared at 1600°C for 5 h in air. The unit cell volume of the compounds increased from 0.853 to 0.878 nm^3 with x . Phase transitions having a temperature hysteresis were observed from 1100° to 1400°C by calorimetry and dilatometry. The transition temperature increased with x . The volume of the high-temperature phase was 0.5% smaller than that of the low-temperature phase at the transition temperature. The volume changes were independent of x . The hysteresis width observed by the dilatometry was about 300°C for the $\text{Gd}_4\text{Al}_2\text{O}_9$ ceramics (grain size: about $1\text{ }\mu\text{m}$) and decreased to 50°C for the $\text{Gd}_4(\text{Al}_{0.2}\text{Ga}_{0.8})_2\text{O}_9$ ceramics (grain size: over $10\text{ }\mu\text{m}$). $\text{Gd}_4\text{Ga}_2\text{O}_9$ was unstable at low temperature and decomposed to Gd_3GaO_6 and $\text{Gd}_3\text{Ga}_5\text{O}_{12}$ during the thermal analyses. © 2001 Kluwer Academic Publishers

1. Introduction

The volume of materials usually increases at the phase transition from a low-temperature phase to a high-temperature phase. Zirconia (ZrO_2) is a well-known exception in oxides [1, 2]. It has a martensitic phase transition around 1000°C with a large temperature hysteresis. The volume of the high-temperature phase is about 3% smaller than that of the low-temperature phase. Ceramics having a phase transition toughening mechanism have been developed by using ZrO_2 .

$\text{Y}_4\text{Al}_2\text{O}_9$ is another oxide which exhibits a volume shrinkage of about 0.5% at the phase transition around 1370°C [3–5]. Recently, the crystal structure of the high-temperature phase was determined by high-temperature neutron diffraction [6]. The space groups of the high-temperature and low-temperature phases are identical, $P2_1/c$. The positional parameters of all the atoms shifted about $1/4$ along the a -axis at the phase transition. Diffusionless, displacive movement of the atoms on the (010) plane clearly demonstrated the martensitic phase transition of $\text{Y}_4\text{Al}_2\text{O}_9$.

Similar phase transitions were reported for rare-earth aluminates, $\text{RE}_4\text{Al}_2\text{O}_9$ ($\text{RE} = \text{Sm}, \text{Eu}, \text{Gd}, \text{Tb}, \text{Dy}, \text{Ho}, \text{Er}, \text{Tm}, \text{Yb}$) and gallates, $\text{RE}_4\text{Ga}_2\text{O}_9$ ($\text{RE} = \text{La}, \text{Pr}, \text{Nd}, \text{Sm}, \text{Eu}, \text{Gd}$) [7]. The phase transition temperatures increased with the increasing atomic number of RE (decreasing RE^{3+} ionic radius) from 1044° (Sm) to 1300°C (Yb) for the aluminates and from 1271° (La) to 1412°C (Gd) for the gallates. The phase transition temperatures of the aluminates were about 300°C lower than those of the gallates with the same RE.

$\text{RE}_4\text{Al}_2\text{O}_9$ and $\text{RE}_4\text{Ga}_2\text{O}_9$ as well as $\text{Y}_4\text{Al}_2\text{O}_9$ are isostructural with $\text{Ca}_4\text{Si}_2\text{O}_7\text{F}_2$ (cuspidine). The rare-

earth elements are coordinated by 6 or 7 oxygen atoms. Oxygen tetrahedra containing Al or Ga form Al_2O_7 or Ga_2O_7 , respectively, by sharing the apical oxygen atom. In the present paper, the phase transition of the solid solution compounds, $\text{Gd}_4(\text{Al}_{1-x}\text{Ga}_x)_2\text{O}_9$, was investigated in order to clarify the effect of the Al-Ga substitution at the tetrahedral sites of the crystal structure with respect to the phase transition.

2. Experimental

Gd_2O_3 powder (99.99% purity, Mitsubishi Kasei Co.), Al_2O_3 powder (99.99% purity, Sumitomo Chemical Ind.) and Ga_2O_3 powder (99.99% purity, Rare Metallic Co., Ltd.) were used as the starting materials. These powders were weighed with compositions of $\text{Gd}:(\text{Al}_{1-x}\text{Ga}_x) = 2:1$ molar ratio, where $x = 0.0, 0.2, 0.4, 0.6, 0.8$ and 1.0 , and then mixed with an appropriate amount of ethanol in an agate mortar. The mixed powders were pressed into bars ($8 \times 4 \times 30\text{ mm}^3$) at 70 MPa. The bars were heated on a Pt 70% - Rh 30% plate at 1600°C for 5 h in air in a furnace with a molybdenum silicide heater. After heating, the reaction sintered samples were cooled in the furnace by shutting off the electric power. The samples were powdered for X-ray diffraction (XRD) and differential calorimetry (DSC).

The XRD patterns were measured at room temperature on a diffractometer (Rigaku, RINT 2500) using $\text{Cu K}\alpha$ radiation with a pyrolytic graphite monochromator. The intensity data for the Rietveld analysis were collected from $10\text{--}80^\circ$ in 2θ with sampling steps of 0.04° . The Rietveld analysis was performed using the program

* Author to whom all correspondence should be addressed.

“RIETAN” [8]. The atomic parameters of $\text{Y}_4\text{Al}_2\text{O}_9$ reported by Christensen and Hazell [9] were used for the initial values of the Rietveld refinement.

The powdered samples weighing about 50 mg were characterized using a high-temperature differential scanning calorimeter (DSC, Mac Science, DSC3300). The rate of heating and cooling was $20^\circ\text{C}/\text{min}$. Thermal expansion was measured in a dilatometer (Shimadzu, TMA-50) using specimens with a length of about 15 mm. An alumina ceramic rod was used as the standard sample which was calibrated with a sapphire standard. The specimens were heated and cooled in air at the rate of $20^\circ\text{C}/\text{min}$. The fracture surface of the reaction sintered samples was observed with a scanning electron microscope (Hitachi, S-1250).

3. Results and discussion

Fig. 1 shows as an example the profile fit and difference patterns of the Rietveld analysis for the X-ray powder diffraction data of $\text{Gd}_4(\text{Al}_{0.2}\text{Ga}_{0.8})_2\text{O}_9$. The solid lines are calculated intensity profiles, and the dots crossing the profiles are observed intensities. The short vertical lines show the possible Bragg reflections. The differences between the observed and calculated intensities are plotted below the profiles. The positional parameters of the Gd atoms were well refined. However, the parameters of the other lighter atoms could not be uniquely refined with reasonable interatomic distances because of the weak X-ray scattering power of these atoms compared to that of the Gd atoms. The final R -factors of the Rietveld analysis for the samples with $x = 0.0$ – 0.8 were 10–13% for R_{wp} , 2–3% for R_1 and R_F , and 1.2–1.3 for S . Very small diffraction peaks from Gd_3GaO_6 and $\text{Gd}_3\text{Ga}_5\text{O}_{12}$ were included in the XRD pattern of the sample $x = 1.0$. The final R -factors of the Rietveld analysis of this XRD pattern without any data exclusion were $R_{\text{wp}} = 17\%$, $R_p = 13.31$, $S = 1.61$, $R_1 = 7.34$, and $R_F = 4.54\%$.

The lattice parameters of $\text{Gd}_4(\text{Al}_{1-x}\text{Ga}_x)_2\text{O}_9$ are plotted in Fig. 2. The a -axis length at $x = 0.1$, 0.2 and 0.3 dropped about 0.10–0.06% from the length of $x = 0.0$. The a -axis lengths of the other samples increased with x . The parameters of the b and c axes increased monotonously with x . The β angles decreased with x were almost on a straight line. The cell volumes calculated with these parameters increased with x . The influence of the drop in the a -axis length at $x = 0.1$ – 0.3 to the cell volume was small. We tried to refine the crystal structure of $\text{Gd}_4(\text{Al}_{0.8}\text{Ga}_{0.2})_2\text{O}_9$ with a model of preferential substitution at one of the two Al sites for Ga and with a model of statistical substitution at the two sites. However, we could not conclude any explicit difference between the results using these two models. All refinements of the other samples were carried out with the statistical substitution model.

DSC curves measured for $\text{Gd}_4(\text{Al}_{0.2}\text{Ga}_{0.8})_2\text{O}_9$ above 1260°C are shown in Fig. 3 as an example. No calorimetric change was detected below this temperature. During the two cycles of heating and cooling, endothermic peaks were observed at 1396°C on heating and exothermic peaks at 1353°C on cooling. Similar DSC curves were obtained for the other samples. Fig. 4 shows the transition temperatures defined as the average of the exothermic and endothermic peak temperatures. The hysteresis widths between these peaks are also shown in this figure. The transition temperature increased from 1104° to 1400°C and the widths gradually decreased from 109° to 35°C with increasing x .

Fig. 5 shows the dilatometry of the ceramic samples. For the sample of $x = 0.0$, the volume shrinkage of the phase transition was observed from 1099° to 1230°C on heating, and the volume expansion occurred from 1001° to 880°C on cooling. The averages of the mean temperatures for the start and finish of the volume change on heating and cooling were plotted in Fig. 4 as the phase transition temperatures from the dilatometry. These transition temperatures deviated from the

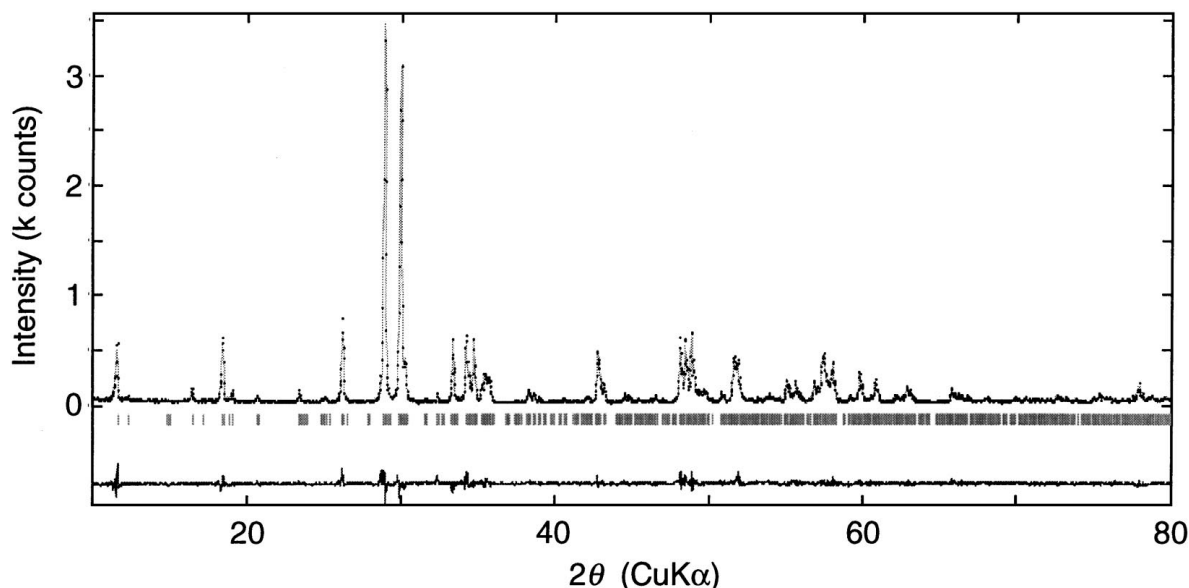


Figure 1 Rietveld refinement profile of the X-ray diffraction pattern for $\text{Gd}_4(\text{Al}_{0.2}\text{Ga}_{0.8})_2\text{O}_9$. The dotted line represents the observed intensities. Difference plots are shown beneath the patterns. Positions of the Bragg reflections are represented by vertical bars.

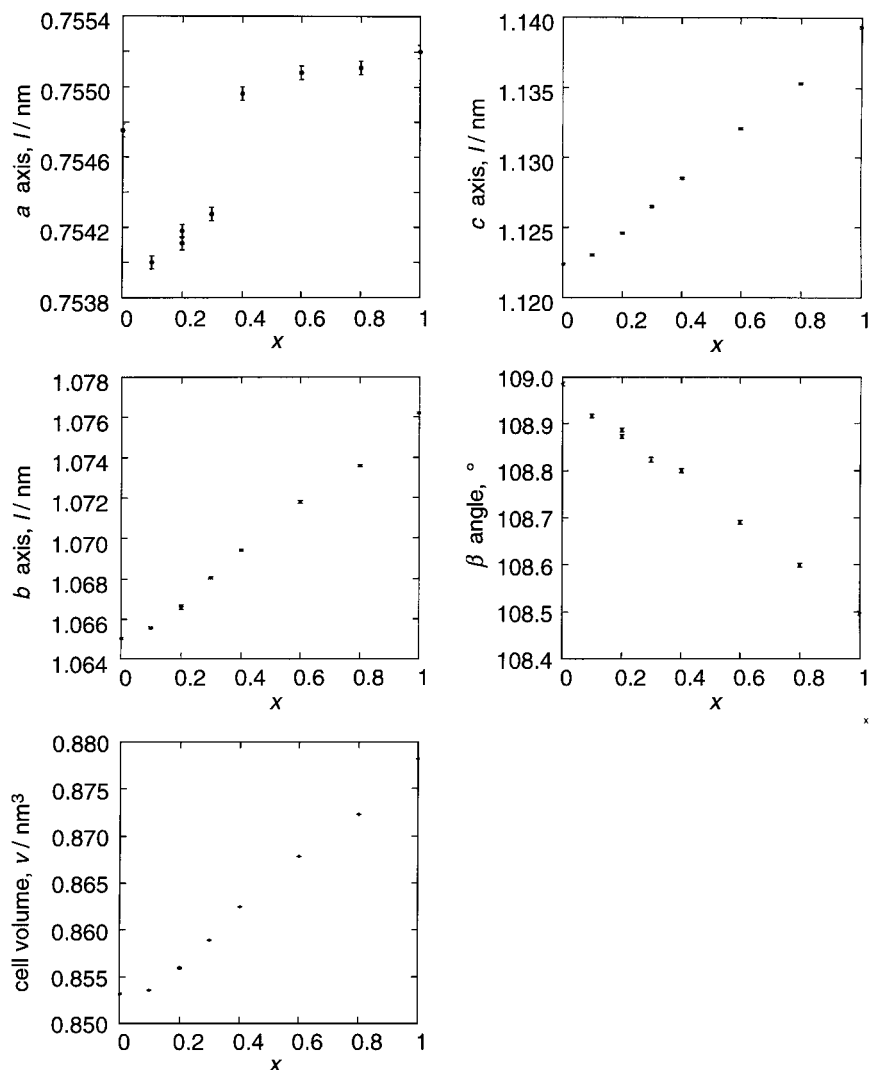


Figure 2 The lattice parameters and cell volume of $Gd_4(Al_{1-x}Ga_x)_2O_9$ versus x .

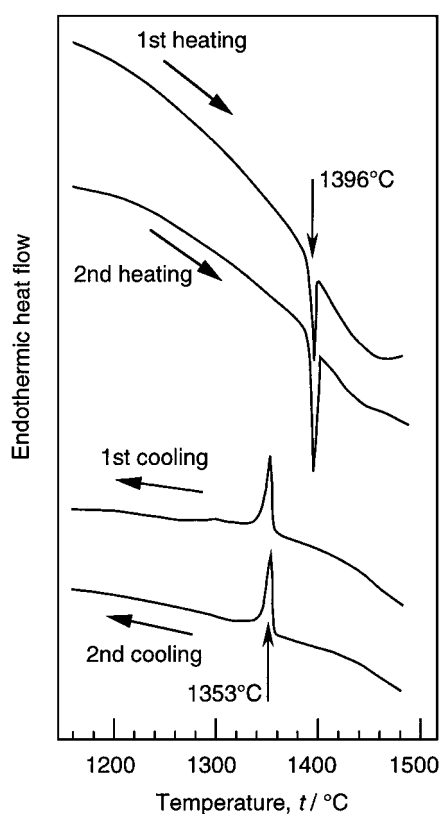


Figure 3 DSC curves of $Gd_4(Al_{0.2}Ga_{0.8})_2O_9$.

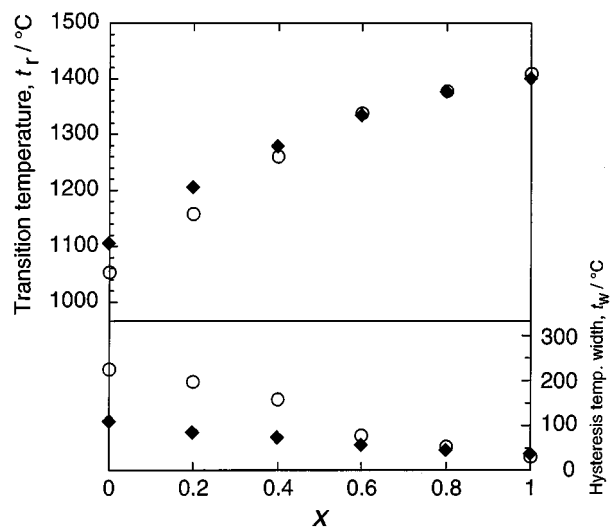


Figure 4 Transition temperature and hysteresis width of $Gd_4(Al_{1-x}Ga_x)_2O_9$ measured by DSC (◆) and DLT (○).

temperatures determined by the DSC for small x values. The hysteresis widths of the ceramic samples are shown in Fig. 4 with the difference between the mean temperatures on heating and cooling. The hysteresis width was 224°C at $x = 0.0$ ($Gd_4Al_2O_9$) and decreased to 32°C at $x = 0.8$. The difference between the cell volumes of the high- and low-temperature phases

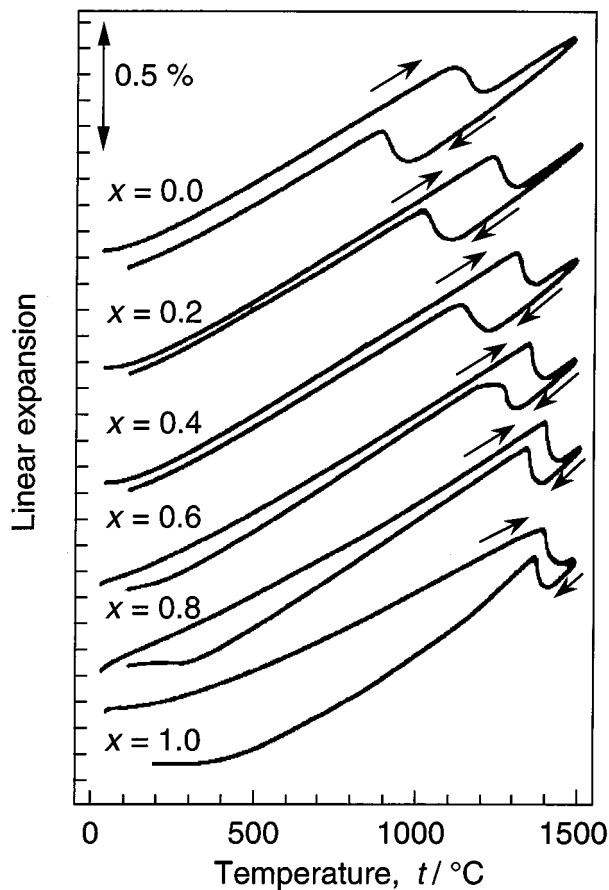


Figure 5 Dilatometry curves of the $Gd_4(Al_{1-x}Ga_x)_2O_9$ ceramics.

at the transition temperatures was about 0.5% for all samples.

As seen in the SEM photographs of Fig. 6a, the grain size of the $Gd_4Al_2O_9$ ceramics was about $1 \mu m$. The grain size of the sample with $x = 0.2$ was about $3 \mu m$. In the sample with $x = 0.8$, the grains grew to over $10 \mu m$. The enhancement in the grain growth was related to the solidification point of $Gd_4Ga_2O_9$ ($1780^\circ C$) [10, 11] which was lower than that of $Gd_4Al_2O_9$ ($1951^\circ C$) [12]. The large hysteresis of the phase transition was related to the grain size. A similar grain size dependence was observed in the previous study for $Y_4Al_2O_9$ ceramics [4] as well as in the studies on ZrO_2 ceramics [1]. The samples composed of smaller grains exhibited a larger hysteresis. The martensitic transition accompanying the shear stress could be restricted at the boundary of the grains with a relatively large surface area versus the volume.

A large shrink was observed for the sample of $x = 1.0$ (Fig. 6), in particular, on cooling. After the dilatometry measurement, the intensity of the peaks from Gd_3GaO_6 and $Gd_3Ga_5O_{12}$ increased in the XRD pattern. This result was in accordance with the phase diagram of Gd_2O_3 - Ga_2O_3 [10]. $Ga_4Ga_2O_9$ is unstable below $1400^\circ C$. $Gd_3Ga_5O_{12}$ has a garnet-type structure. The space group of Gd_3GaO_6 was reported to be $Pnna$ from the previous studies [10, 13]. However, the crystal structure of this compound was recently determined to have the space group $Cmc2_1$ ($a = 0.8993$, $b = 1.1281$, $c = 0.54812$ nm), isostructural with Er_3GaS_6 [14]. No change was observed in

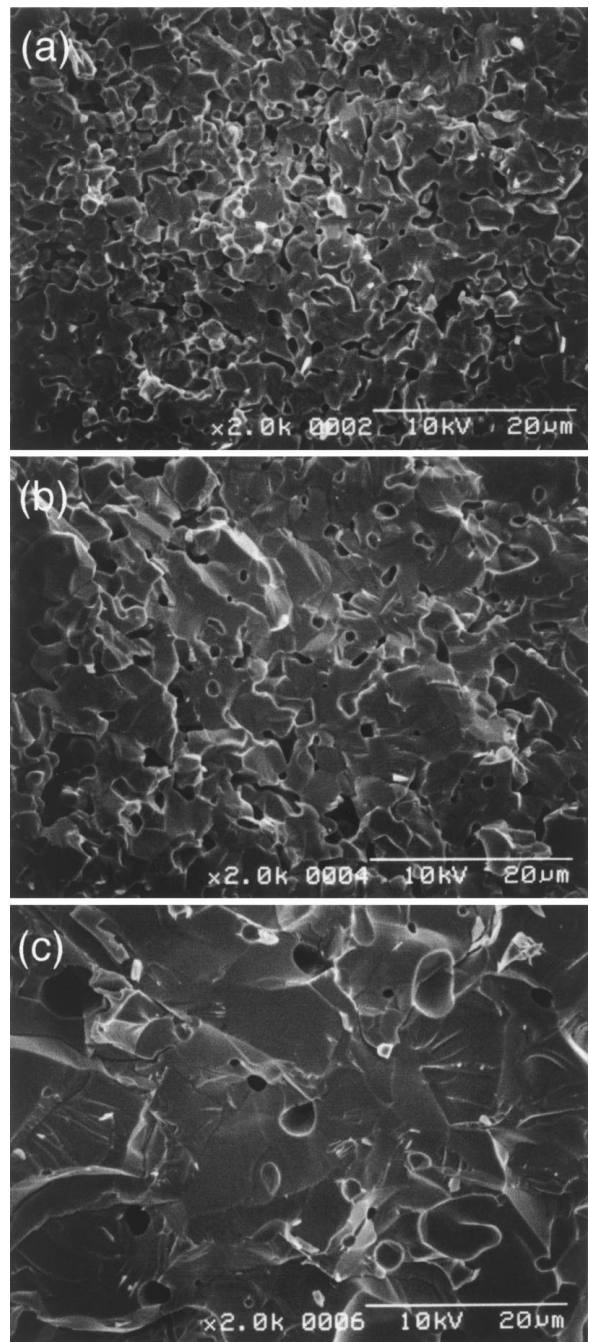


Figure 6 Scanning electron micrographs of $Gd_4(Al_{1-x}Ga_x)_2O_9$; $x = 0.0$ (a), 0.2 (b) and 0.8 (c).

the XRD patterns for the samples with $x = 0.0$ – 0.8 after the dilatometry measurements.

A small hysteresis was observed from room temperature to about $1000^\circ C$ for the samples $x = 0.6$ and 0.8 . A similar thermal hysteresis was observed for the $Y_4Al_2O_9$ ceramics with large grains [4]. This hysteresis was explained by crack formation on cooling and crack healing at high temperature. The microcracks were introduced into the ceramics due to the anisotropic thermal expansion of $Y_4Al_2O_9$. The same explanation could be adopted for the hysteresis of $Gd_4(Al_{1-x}Ga_x)_2O_9$ ceramics composed of large grains.

4. Conclusion

Solid solutions of $Gd_4(Al_{1-x}Ga_x)_2O_9$ were prepared by the solid state reaction at $1600^\circ C$ for 5 h in air. The

phase transition of the solid solutions with $x = 0.2-0.8$ occurred not at the transition temperatures of $Gd_4Al_2O_9$ and $Gd_4Ga_2O_9$ but at a temperature between the transition temperatures of these terminal phases. The transition temperature increased with x . The unit cell volumes or probably the size of the two tetrahedra of $(Al,Ga)_2O_7$ in the structure is important to control the martensitic phase transition temperature of $Gd_4(Al_{1-x}Ga_x)_2O_9$.

Acknowledgements

This work was partly supported by the Ministry of Education, Science, Sports and Culture Japan, by the Nippon Sheet Glass Foundation for Materials Science and Engineering, and by NEDO under the Synergy Ceramics Project of the Industrial Science and Technology Frontier Program promoted by AIST, MITI, Japan. M. S. is a member of the Joint Research Consortium of Synergy Ceramics.

References

1. E. C. SUBBARAO, in "Science and Technology of Zirconia," edited by A. H. Heuer and L. W. Hobbs (The American Ceramic Society, Inc. Columbus, Ohio, 1981) p. 1.
2. D. J. GREEN, R. H. J. HANNINK and M. V. SWAIN,

- in "Transformation Toughening of Ceramics" (CRC Press, Boca Raton, Florida, 1989) p. 1.
3. H. YAMANE, M. OMORI, A. OKUBO and T. HIRAI, *J. Amer. Ceram. Soc.* **76** (1993) 2382.
4. H. YAMANE, K. OGAWARA, M. OMORI and T. HIRAI, *ibid.* **78** (1995) 1230.
5. H. YAMANE, M. OMORI and T. HIRAI, *J. Mater. Sci. Lett.* **14** (1995) 470.
6. H. YAMANE, M. SHIMADA and B. A. HUNTER, *J. Solid State Chem.* **141** (1998) 466.
7. H. YAMANE, K. OGAWARA, M. OMORI and T. HIRAI, *J. Amer. Ceram. Soc.* **78** (1995) 2385.
8. F. IZUMI, in "The Rietveld Method," edited by R. A. Young (Oxford University Press, New York, 1993) p. 236.
9. A. N. CHRISTENSEN and R. G. HAZELL, *Acta Chimica Scandinavia* **45** (1991) 226.
10. J. NICOLAS, J. COUTURES and J. P. COUTRUES, *J. Solid State Chem.* **52** (1984) 101.
11. M. MIZUNO and T. YAMADA, *Yogyo-Kyokai-Shi* **93** (1985) 686.
12. M. MIZUNO, T. YAMADA and T. NOGUCHI, *ibid.* **85** (1977) 543.
13. J. COUTRES, J. NICOLAS, E. ANTIC, G. SCHIFFMACHER and J. COUTURES, *C. R. Acad. Sc. Paris t.* **296** (1983) 347.
14. H. YAMANE, T. SAKAMOTO, S. KUBOTA and M. SHIMADA, *Acta Cryst.* **C55** (1999) 479.

Received 11 February
and accepted 21 June 2000